

Strategies to Explore and Develop Reversible Redox Reactions of Li–S in Electrode Architectures Using Silver-Polyoxometalate Clusters

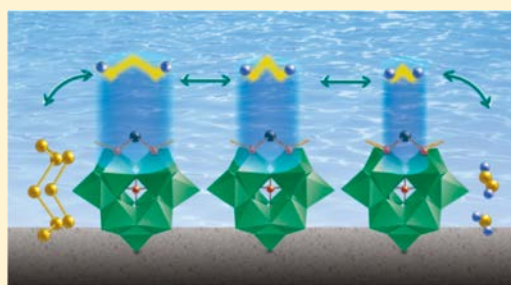
Jian Chuan Ye,^{§,†} Jia Jia Chen,^{§,‡} Ru Ming Yuan,[†] Ding Rong Deng,[†] Ming Sen Zheng,^{*,†} Leroy Cronin,^{*,†,‡} and Quan Feng Dong^{*,†}

[†]Department of Chemistry, College of Chemistry and Chemical Engineering, Collaborative Innovation Centre of Chemistry for Energy Materials, State Key Laboratory of Physical Chemistry of Solid Surfaces, Xiamen University, Xiamen, Fujian 361005, China

[‡]WestCHEM, School of Chemistry, The University of Glasgow, University Avenue, Glasgow G12 8QQ, Scotland (U.K.)

Supporting Information

ABSTRACT: Investigations of the Ag (I)-substituted Keggin $K_3[H_3Ag^I PW_{11}O_{39}]$ as a bifunctional Lewis acidic and basic catalyst are reported that explore the stabilization of Li_2S_n moieties so that reversible redox reactions in S-based electrodes would be possible. Spectroscopic investigations showed that the Li_2S_n -moieties can be strongly adsorbed on the $\{Ag^I PW_{11}O_{39}\}$ cluster, where the Ag(I) ion can act as a Lewis acid site to further enhance the adsorption of the S-moieties, and these interactions were investigated and rationalized using DFT. These results were used to construct an electrode for use in a Li–S battery with a very high S utilization of 94%, and a coulometric capacity of 1580 mAh g^{-1} . This means, as a result of using the AgPOM, both a high active S content, as well as a high areal S mass loading, is achieved in the composite electrode giving a highly stable battery with cycling performance at high rates (1050 and 810 mAh g^{-1} at 1C and 2C over 100 to 300 cycles, respectively).



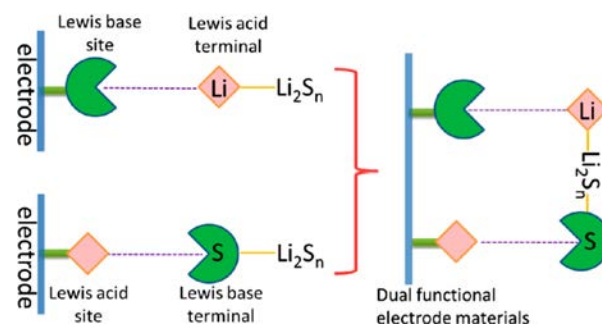
INTRODUCTION

Polyoxometalates (POMs) are anionic clusters linked together by shared oxygen atoms to form well-defined cluster frameworks.^{1–3} Not only do polyoxometalates have an incredible range of interesting redox properties, these have been exploited for possible applications in energy storage systems, such as the active materials for rechargeable batteries^{4–7} and fuel cells.^{8,9} Meanwhile, POMs have potential as efficient catalysts for photocatalysis,^{10,11} and biomass oxidation,^{12,13} as well as promising applications as efficient catalysts for the oxidation of various sulfides.^{14–18} Given that POMs are flexible, electronically active, and derivatizable, we think that there is potential to exploit the superior redox properties of POM clusters to develop new electrode systems. In this context, we hypothesized that it should be possible to develop POM-cluster hybrids for exploring the development of lithium sulfur (Li–S) based redox systems. This is because Li–S batteries are attracting increasing attention due to their high theoretical energy density and specific capacity of up to 2600 Wh kg^{-1} and 1675 mAh g^{-1} , respectively. This is ca. 7 times higher than the maximum capacities of conventional Li-ion batteries which are limited to ca. 250 mAh g^{-1} , and sulfur-based cathodes are believed to be abundant, low cost, and environmental friendly.¹⁹ However, present Li–S batteries are still critically limited by poor S utilization during long battery cycling lifetime due to a severe “shuttle effect”, caused by the formation of unstable higher-order Li_2S_n species in the electrolyte.²⁰ There have been some attempts²¹ to develop new frameworks and matrices to improve the redox reversibility of higher Li_2S_n

species,^{22,23} but the lack of intrinsic redox functionality appears to limit progress. Given these observations, we hypothesized that it might be possible to develop a hybrid metal-oxide system that exploits the idea that the Li in the Li_2S_n species can be regarded as Lewis acidic sites where the polysulfide moieties can be seen as Lewis basic sites (see Scheme 1).

As a result of the high negative charge and large number of terminal oxygen atoms on the external surface of POM clusters, we wondered if a POM hybrid can be used as both a Lewis acidic and Lewis basic site.²⁴ Indeed, the addition of

Scheme 1. Concept Showing How to Limit and Modulate the Absorbance of the Soluble Higher order Li_2S_n Moieties formed in a Li–S Energy Storage System



Received: January 11, 2018

Published: February 9, 2018

heterometal ions like Ag(I) on the skeleton of the polyanion should allow the system to modulate its interactions with sulfides, as well as the terminal oxo-ligands with Li cations.²⁵ As such, we postulated that nanostructured POMs can provide a suitable polar surface to adsorb polysulfides and improve the sulfur utilization and life span of Li–S batteries.^{26,27} For these studies, we hypothesized that a suitably chosen polyoxometalate, like $K_3[H_3Ag^I PW_{11}O_{39}]$,²⁸ would be able to serve as a nanostructured polar inorganic host material with dual Lewis basic and acidic sites. Unlike the introduction of Pt/Au as electro-catalysts to enhance the redox cycling of S-species,²⁹ the use of a POM cluster as electro-catalyst to boost the Li–S battery performance promises to be much cheaper, environmental friendly, and more versatile.

RESULTS AND DISCUSSION

To probe this idea, we developed a model system whereby a hypothetical cluster is associated with a Li_2S_n species and explored both a classical POM and a POM ligated to Ag(I) using DFT (see Figure 1, Table S1 and Figure S1). These

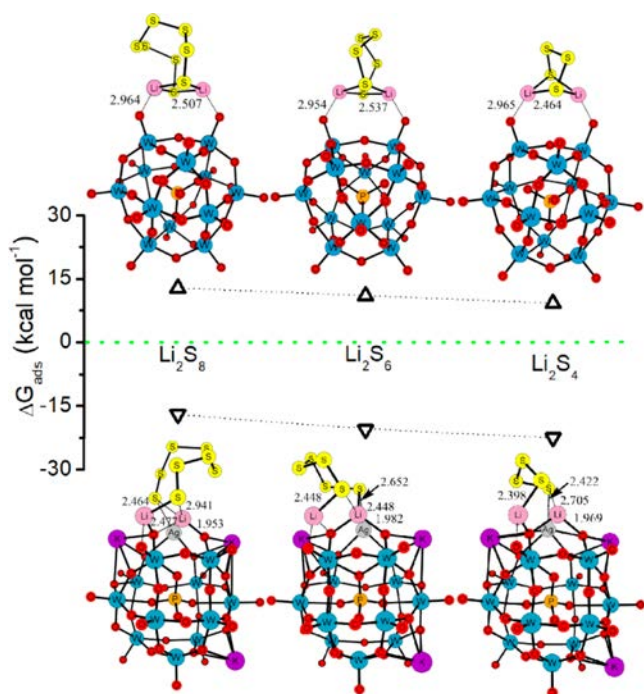


Figure 1. Calculated differences of adsorption free energy, ΔG_{ads} , and optimized structures for Li_2S_n species ($n = 8, 6, 4$) binding with $\{PW_{12}O_{40}\}$ and $\{K_3Ag^I PW_{11}O_{39}\}$ clusters, respectively. $\{PW_{12}O_{40}\}$ is adopted as a control example to explore the role of the Ag ion. Bond lengths are given in Å. Three potassium cations are also factored onto the $\{K_3Ag^I PW_{11}O_{39}\}$ clusters to keep the same negative charges with $\{PW_{12}O_{40}\}$ to ensure a fair comparison. Atoms: (red, oxygen; blue, tungsten; yellow, sulfur; pink, lithium; purple, potassium; gray, silver; and orange, phosphorus).

studies indicated that the Li cations prefer to interact with the bridging oxygen atoms adjacent to the Ag atom of the $\{K_3Ag^I PW_{11}O_{39}\}$ cluster, while the Li_2S_n interacts with the terminal $W = O$ groups on $\{PW_{12}O_{40}\}$ cluster. Both Li atoms in Li_2S_n bind with oxygen atoms of these two clusters, but the $Li \cdots O$ distances in the $\{K_3Ag^I PW_{11}O_{39}\}$ cluster are much shorter than in the $\{PW_{12}O_{40}\}$ cluster (around 1.96 vs 2.95 Å). Moreover, the frontier orbital analysis (Figure S2) shows the

classic POM behavior,^{24,25} where the highest occupied orbital (HOMO) of $\{PW_{12}O_{40}\}$ cluster is delocalized over oxygen atoms all over the cluster while the HOMO of $\{K_3Ag^I PW_{11}O_{39}\}$ cluster is mostly localized around the oxygen atoms adjacent to the Ag atom.

This indicates a much stronger interaction between Li_2S_n and $O = W$ moieties within the $\{K_3Ag^I PW_{11}O_{39}\}$ cluster. Here, the Ag cation ligated in the $\{K_3Ag^I PW_{11}O_{39}\}$ cluster has a Lewis acidic site to interact with the S atoms of the Li_2S_n unit, further enhancing the adsorption. As a result, these studies indicate that the Li_2S_n units can be strongly adsorbed on the $\{K_3Ag^I PW_{11}O_{39}\}$ cluster with ΔG_{ads} of -17.0 to -22.5 kcal mol^{-1} (Table S1). Conversely, the adsorption of Li_2S_n on the $\{PW_{12}O_{40}\}$ cluster is predicted to be energetically unfavorable with a ΔG_{ads} of 9.2 to 12.8 kcal mol^{-1} . These results show that the adsorption of Li_2S_n by dual function sites POM is much stronger than the unsubstituted POM. Furthermore, one of the interactions of the Li–S within the Li_2S_n moiety are elongated by the $\{K_3Ag^I PW_{11}O_{39}\}$ cluster, compared with Li_2S_n on $\{PW_{12}O_{40}\}$ cluster by around 0.11 to 0.43 Å; this is promising since the $\{K_3Ag^I PW_{11}O_{39}\}$ effectively appears to activate the Li_2S_n .

The affinity of Li_2S_n in an electrolyte, like Li_2S_6 , with the $K_3[H_3Ag^I PW_{11}O_{39}]$ clusters was investigated experimentally by the Raman spectroscopy (see Figure 2). This shows that the

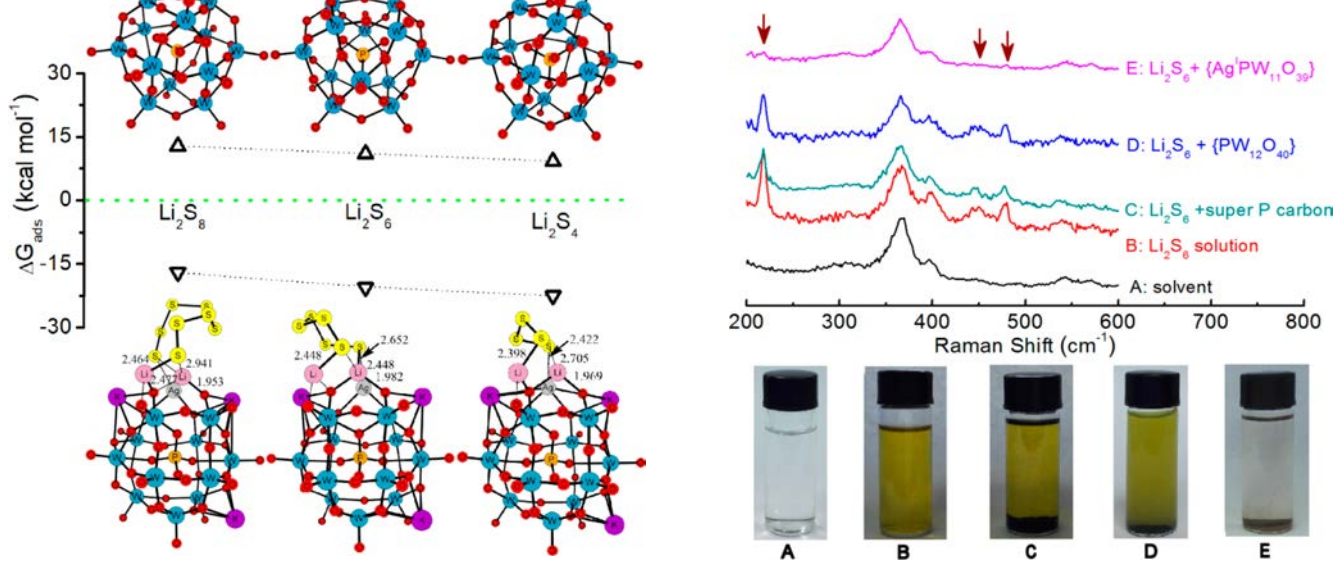


Figure 2. Raman spectra of A (blank solvent of DME/DOXL), B (Li_2S_6 in DME/DOXL solution), C (Li_2S_6 + super P in DME/DOXL solution), D (Li_2S_6 + $\{PW_{12}O_{40}\}$ cluster in DME/DOXL solution), and E (Li_2S_6 + $\{Ag^I PW_{11}O_{39}\}$ cluster in DME/DOXL solution) and their corresponding photographs.

Li_2S_6 has 3 characteristic peaks in the Raman at 218, 447, and 478 cm^{-1} which can be assigned to the bending of δ (SSS), symmetric stretching vibration of $\nu_s(SS)$, and symmetric stretching vibration of (S–SS–S), according to previous Raman studies of sulfides.^{21,30,31} When the solution of Li_2S_6 is mixed with the $\{K_3Ag^I PW_{11}O_{39}\}$ cluster, the yellow Li_2S_6 solution became colorless and the characteristic Raman peaks assigned to the Li_2S_6 disappear. The disappearance of these bands means that the lithium polysulfides in the electrolyte are adsorbed by $K_3[H_3Ag^I PW_{11}O_{39}]$ and are therefore no longer present in the electrolyte. However, the solution characteristics were not altered when the Li_2S_6 solution is mixed with the insoluble

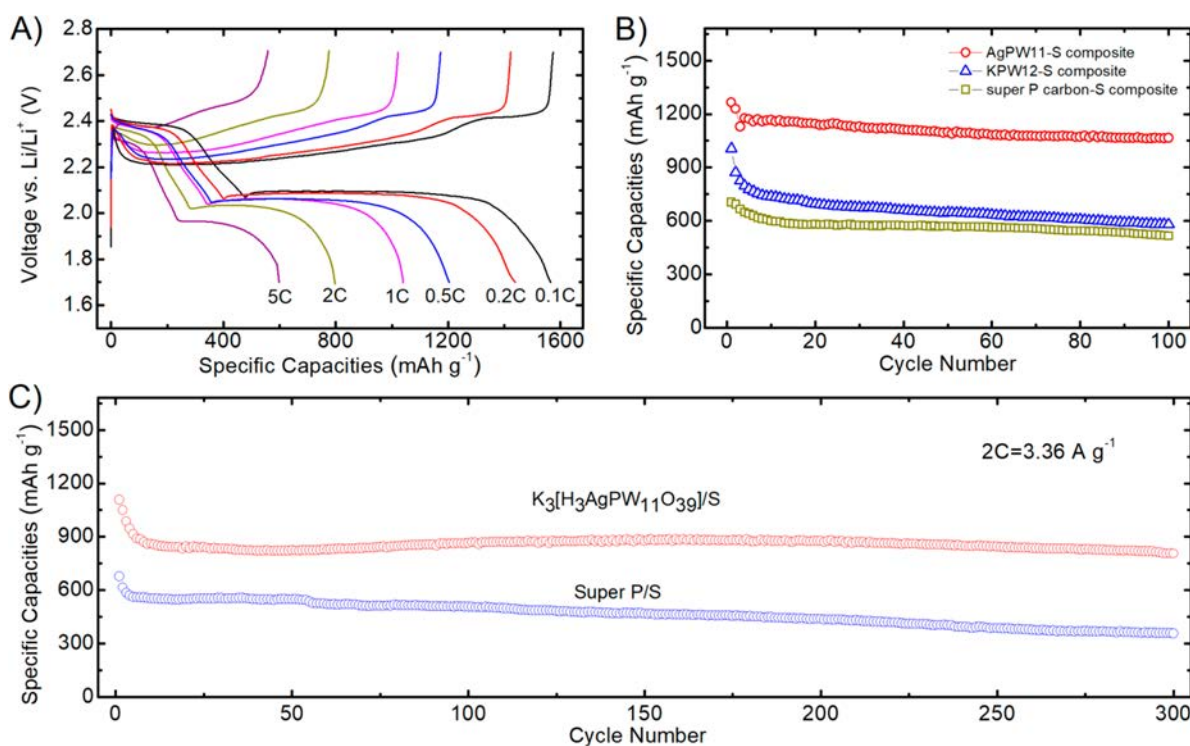


Figure 3. (A) Discharging-charging curves of AgPW₁₁/S cathode at different rates; (B) comparison of battery cycling test of AgPW₁₁/S, K₃PW₁₂O₄₀/S and super P carbon/S for Li–S battery at the rate of 1C (1C = 1.68 A g⁻¹); and (C) long battery cycling of AgPW₁₁/S cathode and super P carbon/S at a higher rate of 2C (2C = 3.36 A g⁻¹). All the above battery data were collected at an active S mass loading of 1.5 mg cm⁻².

super-P carbon and K₃[PW₁₂O₄₀] cluster. Quantitative Raman spectroscopy studies show that K₃[H₃Ag^IPW₁₁O₃₉] clusters can absorb lithium polysulfides effectively (Figures S3 and S4). Moreover, K₃[H₃Ag^IPW₁₁O₃₉] clusters also show an excellent chemical compatibility with lithium polysulfides, and there is no decomposition of the K₃[H₃Ag^IPW₁₁O₃₉] cluster to form Ag₂S (Figure S5).

In addition, the cluster exhibits high structural stability in its dehydrated state where the characteristic rod like structures (with a size of a ca. 300 nm) are retained even after being dehydrated at 250 °C for 10h under a N₂ atmosphere (see SEM image in Figure S6). This is further confirmed by characterization via powder X-ray diffraction and IR spectrometry (Figures S7 and S8). Thus, the K₃[H₃Ag^IPW₁₁O₃₉] POM is highly stable in the dehydrated state before serving as the host material for the S cathode. Motivated by the above results of the adsorption of Li₂S_n species on clusters and theoretical studies, we introduced {K₃Ag^IPW₁₁O₃₉} as an electro-catalyst host material for S cathodes in Li–S batteries. Thus, a AgPW₁₁/S composite cathode, with a high S content (75%), was prepared by heat treatment of a mixture of sulfur and the {K₃Ag^IPW₁₁O₃₉} cluster at 155 °C under N₂ (Figure S9). As observed by SEM analysis (Figure S10), the S penetrates into {Ag^IPW₁₁O₃₉} and coats on the surface of the compound. And this treatment does not influence the chemical state of the sulfur and POMs (Figures S11 and S12). As a control experiment, the same S content and S mass loading of silver-free POM Keggin clusters S cathode and super P carbon/S cathode were also prepared and investigated by the same methodology.

Electrochemical characterization of the AgPW₁₁/S cathode showed two typical discharge plateaus at ca. 2.35 and 2.05 V, respectively (see Figure 3A). The first plateau at 2.35 V can be

attributed to the reduction of S₈ to soluble Li₂S_n (4 ≤ n ≤ 8), and the second plateau at 2.1 V corresponds to the further reduction of Li₂S₄ into solid-state Li₂S₂ and then finally into Li₂S. At the condition of active sulfur mass loading of 1.5 mg cm⁻², the AgPW₁₁/S composites deliver an initial specific capacity of 1580 mAh g⁻¹ at the rate of 0.1C, which corresponds to a high S utilization of 94% compared to the maximum specific theoretical capacity of 1675 mAh g⁻¹. The initial coulombic efficiency is high up to 99.0%, which confirms that the Ag-POM cluster can stabilize the soluble Li₂S_n to retard the irreversible soluble loss, thus a high reversibility can be achieved. Meanwhile, there is no obvious polarization during the discharging when the rates are increased from 0.1 C to 1C, while the specific capacities still can be retained from 1580 to 1050 mAh g⁻¹. A reversible capacity of 600 mAh g⁻¹ can be achieved even when the rate is increased by 50 times to 5 C (corresponding to a current density of 8.4 A g⁻¹). During the discharging-charging process of Li–S battery, the {Ag^IPW₁₁O₃₉} cluster has a negligible electrochemical capacity contribution to the AgPW₁₁/S cathode (Figures S13 and S14). Furthermore, XPS results indicate that the {Ag^IPW₁₁O₃₉} cluster retains its original state within the electrode composite under the working conditions of the Li–S battery (Figure S15).

Moreover, the AgPW₁₁/S composites show a stable and reversible cycling performance at a high rate of 1C, and the specific capacity remains at 1100 mAh g⁻¹ within 100 cycles and the coulombic efficiency of each cycle is nearly 100% (Figure 3B and Figure S16). As a control comparison, the silver-free POM Keggin cluster S cathode shows only a slightly enhanced performance compared to the super P carbon/S cathode. There is only a specific capacity of ca. 1200 mAh g⁻¹ in the first cycle at 0.1C rate (Figure S17) and the capacity degrades continuously to ca. 600 mAh g⁻¹ during the battery cycling at

1C over 100 cycles (Figure 3B). The super P carbon/S cathode also shows a similar capacity degrading to only 500 mAh g⁻¹ after 100 cycles at 1C rate. This result is consistent with our DFT calculations studies above and confirms that the {Ag^IPW₁₁O₃₉} cluster has the ability to improve S utilization and enhance the redox reversibility of S and polysulfides throughout battery cycling. Moreover, AgPW₁₁/S composites exhibit superior long cycling performance even at a higher rate. It also exhibits a durable cycling performance at 2C and keeps a stable capacity of 810 mAh g⁻¹ with nearly 100% coulombic efficiency in 300 cycles (Figure 3C). As a comparison, the super P carbon/S cathode exhibits a continuous capacity degrading to 320 mAh g⁻¹ in 300 cycles.

Although nanostructured polar inorganic compounds have already exhibited an interesting ability to improve the sulfur utilization and cycling life of Li–S batteries, most reports on such cathodes were at a very low S content in the cathode and low areal sulfur loadings (usually lower than 1.0 mg cm⁻² based on the active sulfur).^{32,33} For practical application of Li–S batteries, the areal capacity density should exceed those of today's commercial Li-ion batteries (around 3 mAh cm⁻²).³⁴ Thus, when the areal mass loading of S in the electrode is increased to 3.5 mg cm⁻² (with a E/S mass ratio of 5), it still exhibits a high specific capacity of 1300 mAh g⁻¹ at 0.1C (Figure 4A). This gives a value of 4.55 mAh cm⁻² in terms of areal capacity density which is much higher than the commercial Li-ion batteries.

This further confirms the ability of {Ag^IPW₁₁O₃₉} to strongly interact with lithium polysulfides and should retard the loss of

higher Li₂S_n, increasing the stability and performance of the Li–S battery. Since POMs materials usually have good cation mobility within the clusters, this should also compensate the ionic transfer for AgPW₁₁/S cathodes to exhibit a high rate performance even at a higher S mass loading and a lower E/S mass ratio. As a result, compared with recent work summarized in the literature,³² the AgPW₁₁/S cathode exhibits a much better rate performance with a higher S utilization at a higher S content and a lower amount of electrolyte. Moreover, AgPW₁₁/S cathodes also exhibit excellent rate performance at this high mass loading. Even when the areal current density goes up to 6 mA cm⁻², there is still around a capacity density of 3 mAh cm⁻² (Figure 4A). Furthermore, as shown in Figure 4B, it also shows a stable cycling performance with a specific capacity of 900 mAh g⁻¹ at 0.5 C (corresponding to 3.2 mAh cm⁻² at 2.95 mA cm⁻²) and 780 mAh g⁻¹ at 1C (corresponding to 2.8 mAh cm⁻² at 6 mA cm⁻²). It still exhibits a stable performance at higher rates and longer cycling life with the high S mass loading in the electrode (see Figure S18).

CONCLUSIONS

In summary, we have shown how a silver-POM-based Keggin cluster, {Ag^IPW₁₁O₃₉}, acts as a dual function Lewis acid and base catalyst to boost the battery performance of Li–S batteries. Due to the strong adsorption of Li₂S_n on the {Ag^IPW₁₁O₃₉} cluster, a very high S utilization of 1580 mAh g⁻¹ can be realized at a rate of 0.1 C. In addition, the system shows a highly durable battery cycling performance (1050 mAh g⁻¹ at 1C and 810 mAh g⁻¹ at 2C in 300 cycles). Even when the mass loading of S in the electrode is increased to 3.5 mg cm⁻², the system still shows a high specific capacity of 1300 mAh g⁻¹ at 0.1 C, corresponding to an areal capacity density of 4.55 mAh cm⁻² that is much higher than the present demand of Li-ion batteries. Previously, the poor conductivity of the S cathode was usually thought to be the major limitation in developing Li–S batteries suitable for real world use. However, based on our results with a silver-POM as an adsorption matrix, the vast improvement of the redox reversibility and stability of polysulfides is also an important factor. Finally, considering the potential of other polyoxometalate compounds, we believe that this approach will allow us to develop a new type of high performance Li–S battery driven by polyoxometalate technology.

ASSOCIATED CONTENT

Supporting Information

The Supporting Information is available free of charge on the ACS Publications website at DOI: 10.1021/jacs.8b00411.

Material synthesis, electrochemical characterization, and DFT calculations (PDF)

AUTHOR INFORMATION

Corresponding Authors

*qfdong@xmu.edu.cn;
*lee.cronin@glasgow.ac.uk;
*mszheng@xmu.edu.cn.

ORCID

Jia Jia Chen: 0000-0003-1044-7079

Ru Ming Yuan: 0000-0002-2639-6520

Leroy Cronin: 0000-0001-8035-5757

Quan Feng Dong: 0000-0002-4886-3361

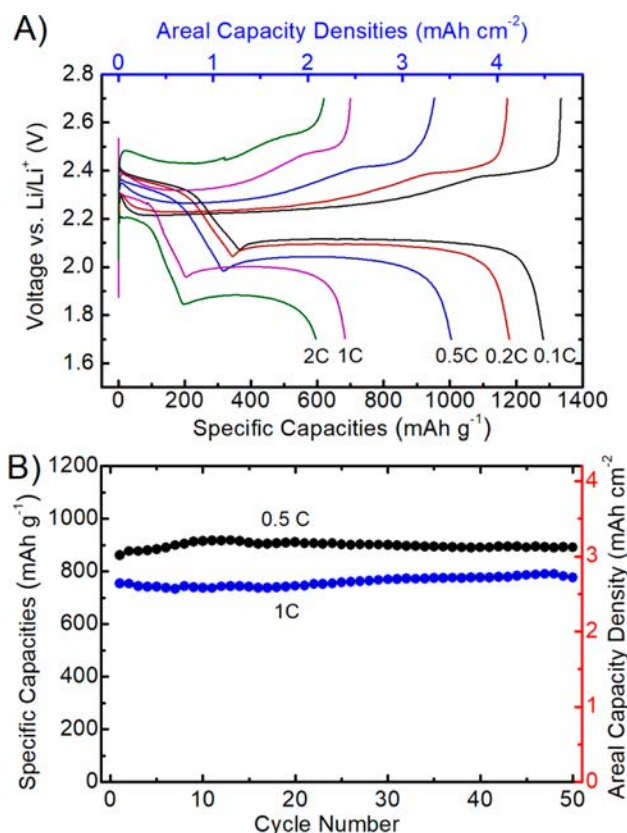


Figure 4. (A) Voltage versus specific capacity and areal capacity densities of AgPW₁₁/S cathode at different rates at the sulfur mass loading of 3.5 mg cm⁻². (B) Battery cycling of AgPW₁₁/S cathode with a sulfur mass loading of 3.5 mg cm⁻² at higher rates of 0.5 C and 1C.

Author Contributions

§J.C.Y. and J.J.C. contributed equally to this work.

Notes

The authors declare no competing financial interest.

ACKNOWLEDGMENTS

We gratefully acknowledge financial support from the National 973 Program (2015CB251102), the Key Project of NSFC (U1305246, 2167319, 21621091, and 21773192), the Fundamental Research Funds for the Central Universities (20720150042 and 20720150043), and EPSRC (Grants EP/J015156/1, EP/K021966/1, EP/K023004/1), ERC (project 670467 SMART-POM). L.C. thanks the National Thousand Talents Program of the PR of China.

REFERENCES

- (1) Miras, H. N.; Yan, J.; Long, D.-L.; Cronin, L. *Chem. Soc. Rev.* **2012**, *41*, 7403.
- (2) Long, D. L.; Yan, J.; Ruiz de la Oliva, A.; Busche, C.; Miras, H. N.; Errington, R. J.; Cronin, L. *Chem. Commun.* **2013**, *49*, 9731.
- (3) Kandasamy, B.; Wills, C.; McFarlane, W.; Clegg, W.; Harrington, R. W.; Rodríguez-Fortea, A.; Poblet, J. M.; Bruce, P. G.; Errington, R. *J. Chem. - Eur. J.* **2012**, *18*, 59.
- (4) Chen, J. J.; Symes, M. D.; Fan, S. C.; Zheng, M. S.; Miras, H. N.; Dong, Q. F.; Cronin, L. *Adv. Mater.* **2015**, *27*, 4649.
- (5) Nishimoto, Y.; Yokogawa, D.; Yoshikawa, H.; Awaga, K.; Irle, S. *J. Am. Chem. Soc.* **2014**, *136*, 9042.
- (6) Wang, H.; Hamanaka, S.; Nishimoto, Y.; Irle, S.; Yokoyama, T.; Yoshikawa, H.; Awaga, K. *J. Am. Chem. Soc.* **2012**, *134*, 4918.
- (7) Ji, Y.; Huang, L.; Hu, J.; Streb, C.; Song, Y. F. *Energy Environ. Sci.* **2015**, *8*, 776.
- (8) Ma, H.; Liu, B.; Li, B.; Zhang, L.; Li, Y.-G.; Tan, H.-Q.; Zang, H.-Y.; Zhu, G. *J. Am. Chem. Soc.* **2016**, *138*, 5897.
- (9) Zang, H. Y.; Chen, J. J.; Long, D. L.; Cronin, L.; Miras, H. N. *Adv. Mater.* **2013**, *25*, 6245.
- (10) Herrero, C.; Quaranta, A.; Leibl, W.; Rutherford, A. W.; Aukauloo, A. *Energy Environ. Sci.* **2011**, *4*, 2353.
- (11) Park, H.; Kim, H. i.; Moon, G. h.; Choi, W. *Energy Environ. Sci.* **2016**, *9*, 411.
- (12) Albert, J.; Wolfel, R.; Bosmann, A.; Wasserscheid, P. *Energy Environ. Sci.* **2012**, *5*, 7956.
- (13) Reichert, J.; Brunner, B.; Jess, A.; Wasserscheid, P.; Albert, J. *Energy Environ. Sci.* **2015**, *8*, 2985.
- (14) Wang, S. S.; Yang, G. Y. *Chem. Rev.* **2015**, *115*, 4893.
- (15) Mirhoseini, H.; Taghdiri, M. *Fuel* **2016**, *167*, 60.
- (16) Yang, C. B.; Jin, Q. P.; Zhang, H.; Liao, J.; Zhu, J.; Yu, B.; Deng, J. G. *Green Chem.* **2009**, *11*, 1401.
- (17) Kamata, K.; Hirano, T.; Mizuno, N. *Chem. Commun.* **2009**, *26*, 3958.
- (18) Kamata, K.; Hirano, T.; Ishimoto, R.; Mizuno, N. *Dalton Trans.* **2010**, *39*, 5509.
- (19) Gao, X. P.; Yang, H. X. *Energy Environ. Sci.* **2010**, *3*, 174.
- (20) Mikhaylik, Y. V.; Akridge, J. R. *J. Electrochem. Soc.* **2004**, *151*, A1969.
- (21) Chen, J. J.; Yuan, R. M.; Feng, J. M.; Zhang, Q.; Huang, J. X.; Fu, G.; Zheng, M. S.; Ren, B.; Dong, Q. F. *Chem. Mater.* **2015**, *27*, 2048.
- (22) Li, Y.-J.; Fan, J.-M.; Zheng, M.-S.; Dong, Q.-F. *Energy Environ. Sci.* **2016**, *9*, 1998.
- (23) Zheng, J.; Tian, J.; Wu, D.; Gu, M.; Xu, W.; Wang, C.; Gao, F.; Engelhard, M. H.; Zhang, J.-G.; Liu, J.; Xiao, J. *Nano Lett.* **2014**, *14*, 2345.
- (24) Lopez, X.; Carbo, J. J.; Bo, C.; Poblet, J. M. *Chem. Soc. Rev.* **2012**, *41*, 7537.
- (25) Poblet, J. M.; Lopez, X.; Bo, C. *Chem. Soc. Rev.* **2003**, *32*, 297.
- (26) Pang, Q.; Kundu, D.; Cuisinier, M.; Nazar, L. *Nat. Commun.* **2014**, *5*, 4759.

(27) An, T.; Deng, D.; Lei, M.; Wu, Q. H.; Tian, Z.; Zheng, M.; Dong, Q. *J. Mater. Chem. A* **2016**, *4*, 12858.

(28) Cui, Y.; Shi, L.; Yang, Y.; You, W.; Zhang, L.; Zhu, Z.; Liu, M.; Sun, L. *Dalton Trans.* **2014**, *43*, 17406.

(29) Al Salem, H.; Babu, G.; Rao, C. V.; Arava, L. M. R. *J. Am. Chem. Soc.* **2015**, *137*, 11542.

(30) Janz, G. J.; Coutts, J. W.; Downey, J. R., Jr.; Roduner, E. *Inorg. Chem.* **1976**, *15*, 1755.

(31) Hagen, M.; Schiffels, P.; Hammer, M.; Dorfner, S.; Tubke, J.; Hoffmann, M. J.; Althues, H.; Kaskel, S. *J. Electrochem. Soc.* **2013**, *160*, A1205.

(32) Liu, X.; Huang, J.-Q.; Zhang, Q.; Mai, L. *Adv. Mater.* **2017**, *29*, 1601759.

(33) Peng, H.-J.; Huang, J.-Q.; Cheng, X.-B.; Zhang, Q. *Adv. Energy Mater.* **2017**, *7*, 1700260.

(34) Sun, H.; Mei, L.; Liang, J.; Zhao, Z.; Lee, C.; Fei, H.; Ding, M.; Lau, J.; Li, M.; Wang, C.; Xu, X.; Hao, G.; Papandrea, B.; Shakir, L.; Dunn, B.; Huang, Y.; Duan, X. *Science* **2017**, *356*, 599.